Electronic and phononic states of the Holstein-Hubbard dimer of variable length

M. Acquarone
GNSM-CNR, Unità INFM di Parma, Dipartimento di Fisica, Università di Parma, 43100 Parma, Italy

J. R. Iglesias and M. A. Gusmão
Instituto de Física, Universidade Federal do Rio Grande do Sul, 91501-970 Porto Alegre, RS, Brazil

C. Noce and A. Romano
Unitá INFM di Salerno, Dipartimento di Fisica Teorica e SMSA, Universitàdi Salerno, 84081 Baronissi, Salerno, Italy

(Received 30 December 1997; revised manuscript received 4 June 1998)

We consider a model Hamiltonian for a dimer of length a including all the electronic one- and two-body terms consistent with a single orbital per site, a free Einstein phonon term for a frequency Ω, and an electron-phonon coupling g_0 of the Holstein type. The bare electronic interaction parameters were evaluated in terms of Wannier functions built from Gaussian atomic orbitals. An effective polaronic Hamiltonian was obtained by an unrestricted displaced-oscillator transformation, followed by evaluation of the phononic terms over a squeezed-phonon variational wave function. For the cases of quarter-filled and half-filled orbitals, and over a range of dimer length values, the ground state for given g_0 and Ω was identified by simultaneously and independently optimizing the orbital shape, the phonon displacement, and the squeezing effect strength. As a varies, we generally find discontinuous changes of both electronic and phononic states, accompanied by an appreciable renormalization of the effective electronic interactions across the transitions, due to the equilibrium shape of the wave functions strongly depending on the phononic regime and on the type of ground state.
[S0163-1829(98)06035-4]

I. INTRODUCTION

Much attention has been devoted to materials where structural effects deeply influence the electronic phenomena, such as, for instance, $V_{2-x}Cr_xO_3$,[1] polyacetylene,[2,3] displacive-type ferroelectrics,[4] the manganites exhibiting colossal magnetoresistance,[5] and the high temperature superconducting perovskites.[6–8] From the theoretical standpoint, such effects have been studied by adding various kinds of electron-phonon couplings to different electronic Hamiltonians, mainly of the extended Hubbard or t-J type. However, comparatively little attention has been paid to the effect of the structure (in its simplest form, a variation of the lattice spacing a) onto the electronic interactions themselves. Such effects are of great relevance in experiments: consider, for example, the measurements under either external or chemical pressure, and the wealth of interesting phenomena that they have revealed. The electronic interaction parameters can be written as integrals of various combinations of Wannier functions centered on the lattice sites (as will be detailed in Sec. II below). Therefore, a change of a is expected to have a non-negligible effect on them. In the realm of electronic transitions, to our knowledge, after a pioneering attempt by Kawabata,[9] only Spałek and Wójcik[10] focused on such effects. They argued that, in a system of fermions undergoing a metal-insulator transition (MIT) due to the on-site repulsion effect, the wave functions may significantly change their shape across the transition, concomitantly to a change of the equilibrium lattice spacing. Therefore, different values for the hopping amplitude t_{ij} and the on-site repulsion U may correspond to the itinerant and the localized regimes. In the present work we explore the consequences of such an approach in systems with a Holstein-type electron-phonon interaction. Our model Hamiltonian includes all the electronic interaction parameters for one- and two-body terms, whose dependence on a results from their evaluation in terms of Wannier functions built from Gaussian orbitals. We also consider the characteristic structural length a as free to vary between reasonable boundaries, in order to model the effects of the experimental techniques that allow for a more or less continuous tuning of the bond length. We find that both the electronic and phononic states significantly depend on a. For instance, on one side, the phonon state, characterized by the extent of the *displacement* and the *squeezing*, reflects the electronic transitions at a deeper level than just a frequency renormalization. On the other side, as the optimal shape of the Wannier wave functions depends not only on a, but also on the phonon state, the renormalization of the electronic parameters by the phonons is actually more complex than indicated by the standard results of the polaronic model.[11]

To put into evidence the basic features of our approach, avoiding unnecessary complications, our model system in the present paper is a simple dimer with a single orbital per site. It can be considered as the basic unit to build clusters and lattices, and its simplicity allows for a full control on the analytic aspects of the calculations. Also, some unavoidable approximations that have to be introduced are linked to the physics, and not to the complications of treating larger systems. Some new aspects distinguish the present work from the rich existing literature on the Holstein dimer with various types of interelectronic interactions (see, for instance, Refs. 2, 12, 13, and the literature cited therein). First, the effec-

tive electronic Hamiltonian originates from a first-principles Hamiltonian including the complete set of one- and two-body electronic terms consistent with a single orbital per site. To the best of our knowledge, previous studies considered only a more restricted subset of interactions. Second, we present our results mainly by setting the values of the electron-phonon coupling g_0 and phonon energy $\hbar\Omega$ and taking the dimer length a as the continuously varying controlling parameter. The dependence of the state of the system on its length usually receives little attention even though it is much more easily accessible experimentally than the dependence on the strength of the coupling, which requires delicate chemical manipulations. However, some discussion of the case of fixed length and varying coupling will also be given. We will discuss the cases of quarter- and half-filling of the electron orbitals.

The paper is organized as follows: Sec. II presents the model Hamiltonian and the expressions of the electronic interactions explicitly depending on the dimer length. In Sec. III the effective electronic Hamiltonian is obtained, while in Sec. IV several correlation functions and other quantities of experimental interest are explicitly evaluated. The results of the numerical analysis of our model are presented and commented upon in Sec. V. Finally, some general conclusions are presented in Sec. VI.

II. THE MODEL

For a dimer consisting of identical ions centered at $\mathbf{R}_1$ and $\mathbf{R}_2$ we consider the Hamiltonian $H \equiv H_{\rm el} + H^0_{\rm ph} + H_{\rm ep}$, where $H_{\rm el}$ includes all the electronic one- and two-body terms for a single orbital, $H^0_{\rm ph}$ is the free-phonon term for a single Einstein frequency Ω, and $H_{\rm ep}$ introduces an electron-phonon coupling g_0 of the Holstein type.

In standard notation, we have

$$H_{\rm el} = \epsilon_0 \sum_\sigma (n_{1\sigma} + n_{2\sigma}) - \sum_\sigma [t - X(n_{1,-\sigma} + n_{2,-\sigma})](c^\dagger_{1\sigma} c_{2\sigma} + \text{H.c.}) + U \sum_{i=1,2} n_{i\uparrow} n_{i\downarrow} + V n_1 n_2 - 2J_z S^z_1 S^z_2 - J_{xy}(S^+_1 S^-_2 + \text{H.c.}) + P(c^\dagger_{1\uparrow} c^\dagger_{1\downarrow} c_{2\downarrow} c_{2\uparrow} + \text{H.c.}). \quad (1)$$

The bare electronic parameters ϵ_0, t, X, U, V, and P $(=J_z = J_{xy})$ were evaluated according to Ref. 14, using normalized Gaussian ''orbitals'' $\phi_i(\mathbf{r}) = (2\Gamma^2/\pi)^{3/4} \exp[-\Gamma^2(\mathbf{r} - \mathbf{R}_i)^2]$ $(i = 1,2)$. Their overlap integral is $S \equiv \langle \phi_1 | \phi_2 \rangle = \exp(-\Gamma^2 a^2/2)$, where $a = |\mathbf{R}_1 - \mathbf{R}_2|$ is the length of the dimer. Then the two orthonormalized Wannier functions are

$$\Psi_1(\mathbf{r}) = A_+(S)\phi_1(\mathbf{r}) + A_-(S)\phi_2(\mathbf{r}), \qquad \Psi_2(\mathbf{r}) = A_-(S)\phi_1(\mathbf{r}) + A_+(S)\phi_2(\mathbf{r}), \quad (2)$$

with

$$A_\pm(S) = \frac{1}{2}\left[\frac{1}{\sqrt{1+S}} \pm \frac{1}{\sqrt{1-S}}\right]. \quad (3)$$

In order to calculate the parameters one has to evaluate integrals involving Gaussian functions, which have been discussed in Ref. 15. If the ion charge is $Z|e|$, and defining $\beta = \hbar^2/2m$, $\eta = -Ze^2$, and $F_0(x) \equiv x^{-1/2}\,\text{erf}(x^{1/2})$, we obtain

$$\epsilon_0 = \beta\left[3\Gamma^2 + \frac{a^2\Gamma^4 S^2}{(1-S^2)}\right] + \eta\left(\frac{2\Gamma\sqrt{2/\pi}}{1-S^2}\right)[1 + F_0(2a^2\Gamma^2) - 2S^2 F_0(a^2\Gamma^2/2)], \quad (4)$$

$$t = \beta\left[\frac{a^2\Gamma^4 S}{(1-S^2)}\right] - \eta\left(\frac{2\Gamma\sqrt{2/\pi}}{1-S^2}\right)[2SF_0(a^2\Gamma^2/2) - S - SF_0(2a^2\Gamma^2)], \quad (5)$$

$$X = -e^2\left[\frac{\Gamma/\sqrt{\pi}S}{(1-S^2)^2}\right][1 + 2S^2 + F_0(\Gamma^2 a^2) - 2(1+S^2)F_0(\Gamma^2 a^2/4)], \quad (6)$$

$$U = e^2\left[\frac{\Gamma/\sqrt{\pi}}{(1-S^2)^2}\right][2 - S^2 + 2S^4 + S^2 F_0(\Gamma^2 a^2) - 4S^2 F_0(\Gamma^2 a^2/4)], \quad (7)$$

$$V = e^2\left[\frac{\Gamma/\sqrt{\pi}}{(1-S^2)^2}\right][S^2(1+2S^2) + (2-S^2)F_0(\Gamma^2 a^2) - 4S^2 F_0(\Gamma^2 a^2/4)], \quad (8)$$

$$J_z = J_{xy} = P = e^2\left[\frac{\Gamma/\sqrt{\pi}S^2}{(1-S^2)^2}\right][3 + F_0(\Gamma^2 a^2) - 4F_0(\Gamma^2 a^2/4)]. \quad (9)$$

The parts of the Hamiltonian involving phonons are a free-phonon term $H^0_{\rm ph}$ and a Holstein-type interaction $H_{\rm ep}$, reading

$$H^0_{\rm ph} = \frac{1}{2M}(P_1^2 + P_2^2) + \frac{M\Omega^2}{2}(u_1^2 + u_2^2) \quad (10)$$

and

$$H_{\rm ep} \equiv g \sum_\sigma (n_{1\sigma} u_1 + n_{2\sigma} u_2), \quad (11)$$

where M is the mass of the ions, Ω is the phonon frequency, assumed dispersionless for simplicity (Einstein phonon), and $P_i \equiv -i\hbar\partial/\partial u_i$ is the momentum of the ion at position i. We are considering only longitudinal vibrations of the dimer.

The standard procedure to quantize the phononic Hamiltonian requires the introduction of usual phonon operators

$$a_i \equiv (2M\hbar\Omega)^{-1/2}(M\Omega u_i + iP_i) \tag{12}$$

for each site. Actually, it is more convenient to work with symmetric (s) and antisymmetric (b) combinations

$$\begin{aligned} s &= (a_1 + a_2)/\sqrt{2}, \\ b &= (a_1 - a_2)/\sqrt{2}, \end{aligned} \tag{13}$$

such that the free-phonon Hamiltonian $H_{\rm ph}^0$ can be decomposed as

$$H_{\rm ph}^0 \equiv H_{\rm ph}^{0b} + H_{\rm ph}^{0s} = \hbar\Omega\left(b^\dagger b + \frac{1}{2}\right) + \hbar\Omega\left(s^\dagger s + \frac{1}{2}\right) \tag{14}$$

and the electron-phonon Hamiltonian $H_{\rm ep}$ has two contributions,

$$\begin{aligned} H_{\rm ep}^s &= \hbar\Omega\,\gamma_0(n_1 + n_2)(s^\dagger + s), \\ H_{\rm ep}^b &= \hbar\Omega\,\gamma_0(n_1 - n_2)(b^\dagger + b), \end{aligned} \tag{15}$$

where we have used the notation $n_i \equiv \Sigma_\sigma n_{i\sigma}$, and introduced the coupling energy per unit charge $g_0 \equiv g\sqrt{\hbar/2M\Omega}$, which, conveniently scaled by the phonon energy, yields the dimensionless quantity $\gamma_0 \equiv g_0/\hbar\Omega$. Equations (15) show explicitly the coupling of s with the total charge, and b with the charge transfer.

III. THE EFFECTIVE ELECTRONIC HAMILTONIAN

Following the procedure of Ref. 16, we will obtain the effective electronic (polaronic) Hamiltonian $H_{\rm pol}$ by first performing on H a generalized Lang-Firsov (displaced-oscillator) transformation. Then, in the transformed Hamiltonian, we will take the average of the phononic parts over the squeezed-phonon wave function to eliminate the phonon degrees of freedom.

As we have two different boson operators, s and b, there will be two corresponding generators R_s and R_b, and we have to perform a sequence of two unitary transformations on H. The generators are defined as

$$R_b = \delta\gamma_0(n_1 - n_2)(b^\dagger - b) \tag{16}$$

and

$$R_s = \eta\gamma_0(n_1 + n_2)(s^\dagger - s), \tag{17}$$

where δ and η are so far undetermined parameters, whose value will be fixed later in a convenient way.

Notice that $[R_b, R_s] = 0$. Then, the transformed phonon operators are

$$e^{R_b} b e^{-R_b} = b - \delta\gamma_0(n_1 - n_2) \tag{18}$$

and

$$e^{R_s} s e^{-R_s} = s - \eta\gamma_0(n_1 + n_2). \tag{19}$$

We transform, therefore, $H_{\rm ph}^{0b} + H_{\rm ep}^b$ as

$$e^{R_b}(H_{\rm ph}^{0b} + H_{\rm ep}^b)e^{-R_b} = \hbar\Omega\left(b^\dagger b + \frac{1}{2}\right) + \hbar\Omega(1-\delta)\gamma_0(n_1 - n_2)(b^\dagger + b) - \hbar\Omega\,\delta(2-\delta)\gamma_0^2(n_1 - n_2)^2 \tag{20}$$

and

$$e^{R_s}(H_{\rm ph}^{0s} + H_{\rm ep}^s)e^{-R_s} = \hbar\Omega\left(s^\dagger s + \frac{1}{2}\right) + \hbar\Omega(1-\eta)\gamma_0(n_1 + n_2)(s^\dagger + s) - \hbar\Omega\,\eta(2-\eta)\gamma_0^2(n_1 + n_2)^2. \tag{21}$$

Since the purely electronic terms of the total Hamiltonian commute with the total number of electrons, they are not affected by $\exp(R_s)$, and are, thus, insensitive to the value of η. We then choose $\eta = 1$ in order to eliminate the interaction of electrons with symmetrical phonons from the transformed Hamiltonian [see Eq. (21)]. We cannot do the same with δ, since R_b does affect the purely electronic terms. Our approach consists in treating δ as a variational parameter, to be determined by minimizing the total energy.

The R_b-transformed Fermi operators read

$$\begin{aligned} e^{R_b} c_{1\sigma} e^{-R_b} &= c_{1\sigma}[\mathrm{Ch}(\gamma_0 B) - \mathrm{Sh}(\gamma_0 B)], \\ e^{R_b} c_{2\sigma} e^{-R_b} &= c_{2\sigma}[\mathrm{Ch}(\gamma_0 B) + \mathrm{Sh}(\gamma_0 B)], \end{aligned} \tag{22}$$

where we have defined the anti-Hermitian operator $B \equiv \delta(b^\dagger - b)$, and $\mathrm{Sh}(x)$ and $\mathrm{Ch}(x)$ are the hyperbolic sine and cosine functions. Notice the asymmetry with respect to site exchange due to the fact that the antisymmetric phonon operator has been defined as a difference of local operators in a well defined order [see Eq. (13)].

Using Eqs. (22), we can easily work out the transformation of $H_{\rm el}$ under R_b. Notice that electron number operators remain unchanged, and the only noninvariant terms of $H_{\rm el}$ are

$$e^{R_b}(c_{1\sigma}^\dagger c_{1\sigma} + \mathrm{H.c.})e^{-R_b} = \mathrm{Ch}(2\gamma_0 B)(c_{1\sigma}^\dagger c_{1\sigma} + \mathrm{H.c.}) + \cdots \tag{23}$$

and

TABLE I. Eigenvalues and eigenvectors of the Hamiltonian of Eq. (1) for $N=1,2,3,4$. D is the degeneracy of the state. The labels a,b indicate *antibonding* and *bonding* character, while S and T correspond to *singlet* and *triplet* states. For $N=2$ we have defined $E_U \equiv 2\epsilon_0+U+P$, $E_V \equiv 2\epsilon_0+V+J_{xy}$, $r \equiv \sqrt{(E_U-E_V)^2+16(t-X)^2}$, $\tan(\theta) \equiv -4(t-X)/(E_U-E_V+r)$, and $T=t-2X$.

Filling and energy	D	S,S_z	Eigenvectors
$(N=1)$			
$E_1=\epsilon_0-t$	2	1/2,1/2	$\lvert 1b,\uparrow\rangle=\frac{1}{\sqrt{2}}[c_{1\uparrow}^\dagger+c_{2\uparrow}^\dagger]\lvert 0\rangle$
		1/2,−1/2	$\lvert 1b,\downarrow\rangle=\frac{1}{\sqrt{2}}[c_{1\downarrow}^\dagger+c_{2\downarrow}^\dagger]\lvert 0\rangle$
$E_2=\epsilon_0+t$	2	1/2,1/2	$\lvert 1a,\uparrow\rangle=\frac{1}{\sqrt{2}}[c_{1\uparrow}^\dagger-c_{2\uparrow}^\dagger]\lvert 0\rangle$
		1/2,−1/2	$\lvert 1a,\downarrow\rangle=\frac{1}{\sqrt{2}}[c_{1\downarrow}^\dagger-c_{2\downarrow}^\dagger]\lvert 0\rangle$
$(N=2)$			
$E_{Sb}=\frac{1}{2}(E_U+E_V-r)$	1	0,0	$\lvert Sb\rangle=\frac{1}{\sqrt{2}}[\sin\theta(c_{1\downarrow}^\dagger c_{1\uparrow}^\dagger+c_{2\downarrow}^\dagger c_{2\uparrow}^\dagger)-\cos\theta(c_{1\downarrow}^\dagger c_{2\uparrow}^\dagger+c_{2\downarrow}^\dagger c_{1\uparrow}^\dagger)]\lvert 0\rangle$
$E_{T,\pm1}=2\epsilon_0+V-J_z$	2	1,1(−1)	$\lvert T,\pm1\rangle=c_{1\uparrow(\downarrow)}^\dagger c_{2\uparrow(\downarrow)}^\dagger\lvert 0\rangle$
$E_{T,0}=2\epsilon_0+V-J_{xy}$	1	1,0	$\lvert T,0\rangle=\frac{1}{\sqrt{2}}[c_{2\downarrow}^\dagger c_{1\uparrow}^\dagger-c_{1\downarrow}^\dagger c_{2\uparrow}^\dagger]\lvert 0\rangle$
$E_{\mathrm{CT}}=2\epsilon_0+U-P$	1	0,0	$\lvert \mathrm{CT}\rangle=\frac{1}{\sqrt{2}}[c_{1\downarrow}^\dagger c_{1\uparrow}^\dagger-c_{2\downarrow}^\dagger c_{2\uparrow}^\dagger]\lvert 0\rangle$
$E_{Sa}=\frac{1}{2}(E_U+E_V+r)$	1	0,0	$\lvert Sa\rangle=\frac{1}{\sqrt{2}}[\cos\theta(c_{1\downarrow}^\dagger c_{1\uparrow}^\dagger+c_{2\downarrow}^\dagger c_{2\uparrow}^\dagger)+\sin\theta(c_{1\downarrow}^\dagger c_{2\uparrow}^\dagger+c_{2\downarrow}^\dagger c_{1\uparrow}^\dagger)]\lvert 0\rangle$
$(N=3)$			
$E_{3b\sigma}=3\epsilon_0+U+2V-J_z-T$	2	1/2,1/2	$\lvert 3b,\uparrow\rangle=\frac{1}{\sqrt{2}}[c_{1\uparrow}^\dagger c_{1\downarrow}^\dagger c_{2\uparrow}^\dagger+c_{2\uparrow}^\dagger c_{2\downarrow}^\dagger c_{1\uparrow}^\dagger]\lvert 0\rangle$
		1/2,−1/2	$\lvert 3b,\downarrow\rangle=\frac{1}{\sqrt{2}}[c_{1\uparrow}^\dagger c_{1\downarrow}^\dagger c_{2\downarrow}^\dagger+c_{2\uparrow}^\dagger c_{2\downarrow}^\dagger c_{1\downarrow}^\dagger]\lvert 0\rangle$
$E_{3a}=3\epsilon_0+U+2V-J_z+T$	2	1/2,1/2	$\lvert 3a,\uparrow\rangle=\frac{1}{\sqrt{2}}[c_{1\uparrow}^\dagger c_{1\downarrow}^\dagger c_{2\uparrow}^\dagger-c_{2\uparrow}^\dagger c_{2\downarrow}^\dagger c_{1\uparrow}^\dagger]\lvert 0\rangle$
		1/2,−1/2	$\lvert 3a,\downarrow\rangle=\frac{1}{\sqrt{2}}[c_{1\uparrow}^\dagger c_{1\downarrow}^\dagger c_{2\downarrow}^\dagger-c_{2\uparrow}^\dagger c_{2\downarrow}^\dagger c_{1\downarrow}^\dagger]\lvert 0\rangle$
$(N=4)$			
$E_4=4\epsilon_0+2U+4V-2J_z$	1	0,0	$\lvert 4\rangle=c_{1\uparrow}^\dagger c_{1\downarrow}^\dagger c_{2\uparrow}^\dagger c_{2\downarrow}^\dagger\lvert 0\rangle$

$$e^{R_b}(c_{1\uparrow}^\dagger c_{1\downarrow}^\dagger c_{2\downarrow}c_{2\uparrow}+\mathrm{H.c.})e^{-R_b} = \mathrm{Ch}(4\gamma_0 B)(c_{1\uparrow}^\dagger c_{1\downarrow}^\dagger c_{2\downarrow}c_{2\uparrow}+\mathrm{H.c.})+\cdots, \quad (24)$$

where the dots stand for terms that contain $\mathrm{Sh}(\mathrm{const}\times B)$, which average to zero in the squeezed-phonon state, as discussed below.

To eliminate the phonon operators, we take the average of the transformed Hamiltonian over the squeezed-phonon wave function

$$\lvert\Psi_{\mathrm{sq}}\rangle = e^{-\alpha(bb-b^\dagger b^\dagger)}\lvert 0\rangle_{\mathrm{ph}}. \quad (25)$$

It is then straightforward to show that

$$\langle\Psi_{\mathrm{sq}}\rvert\mathrm{Sh}(n\gamma_0 B)\lvert\Psi_{\mathrm{sq}}\rangle = 0, \quad (26)$$

$$\langle\Psi_{\mathrm{sq}}\rvert\mathrm{Ch}(n\gamma_0 B)\lvert\Psi_{\mathrm{sq}}\rangle = \exp\left[-\frac{1}{2}n^2\delta^2\gamma_0^2 e^{-4\alpha}\right].$$

The result is a polaronic effective Hamiltonian $H_{\rm pol}=H_{\rm el}(\epsilon_0^*,t^*,X^*,U^*,V^*,J_{xy}^*,J_z^*,P^*)+E_{\rm ph}$, where

$$\epsilon_0^*=\epsilon-\hbar\Omega\gamma_0^2[1+\delta(2-\delta)],\quad t^*=\tau t,\quad X^*=\tau X,$$
$$U^*=U-2\hbar\Omega\gamma_0^2[1+\delta(2-\delta)],$$
$$V^*=V-2\hbar\Omega\gamma_0^2[1-\delta(2-\delta)],\quad P^*=\tau^4 P,\tag{27}$$
$$E_{\rm ph}=\hbar\Omega[\mathrm{Sh}^2(2\alpha)+1],$$

with $\tau\equiv\exp[-2\delta^2\gamma_0^2e^{-4\alpha}]$. The parameters J_z and J_{xy} remain unchanged (thus, they are no longer equal to P^*). Notice that the energy of the phonons in the ground state is given by the last term in Eq. (27). Leaving aside $\hbar\Omega/2$, coming from the s phonons, the contribution of the b phonons to this energy can be written as

$$E_{\rm ph}^b=\frac{1}{2}\hbar\Omega\ \mathrm{Ch}(4\alpha).\tag{28}$$

Thus, due to the squeezing effect, we find an increase of the zero-point b-phonon energy, as if the frequency of the latter were $\Omega^*\equiv\Omega\ \mathrm{Ch}(4\alpha)$. This renormalization effect is not directly due to the electronic interactions, since it does not depend explicitly on them. There is, however, an indirect influence due to α being determined by minimization of the total energy, which includes the electronic part.[17]

The polaronic Hamiltonian is easily diagonalized, and its energy eigenvalues and eigenvectors are listed in Table I. Leaving aside differences in notation, these results are consistent with those obtained by other authors.[18,19]

IV. CORRELATION FUNCTIONS

The quantities accessible to measurement, besides the energy eigenvalues, are expressed in the form of various correlation functions (CF), which can be evaluated through the eigenstates of the effective Hamiltonian, listed in Table I. We will indicate by $\langle\langle X\rangle\rangle_{|l\rangle}$ the CF for a generic operator X in one of the eigenstates $|l\rangle$ of the effective Hamiltonian. The double average $\langle\langle X\rangle\rangle_{|l\rangle}$ has to be understood as follows:

$$\langle\langle X\rangle\rangle_{|l\rangle}\equiv\langle l|\langle\Psi_{\rm sq}|e^{R_b}e^{R_s}Xe^{-R_s}e^{-R_b}|\Psi_{\rm sq}\rangle|l\rangle.\tag{29}$$

In particular, $\langle\langle H\rangle\rangle_{|l\rangle}=E_l^*$. We will evaluate a number of correlation functions that have been considered in the literature, whose definitions are briefly clarified below.

The squeezing parameter is directly accessible to experimental measure through the Debye-Waller factor, defined as $F^{\rm DW}\equiv\langle\langle u_i^2\rangle\rangle-\langle\langle u_i\rangle\rangle^2$. Indeed, by using the time-dependent representation of the displacement through the effective Hamiltonian H^*, i.e., $u_i(t)\equiv\exp(iH^*t/\hbar)u_i\exp(-iH^*t/\hbar)$, one obtains

$$F^{\rm DW}=\frac{L^2}{2}[1+e^{4\alpha}],\tag{30}$$

where $L\equiv\sqrt{\hbar/2M\Omega}$ is the characteristic phonon length.

An important quantity is the ratio of the kinetic energy of the interacting system to that on the noninteracting one, defined as

$$F_{|l\rangle}^{\rm kin}\equiv\frac{\left\langle\left\langle t\sum_\sigma(a_{1\sigma}^\dagger a_{2\sigma}+a_{2\sigma}^\dagger a_{1\sigma})\right\rangle\right\rangle_{\gamma_0\neq0}}{\left[\langle l|t\sum_\sigma(a_{1\sigma}^\dagger a_{2\sigma}+a_{2\sigma}^\dagger a_{1\sigma})|l\rangle\right]_{\gamma_0=0}}.\tag{31}$$

For $N=1$, $F_{|l\rangle}^{\rm kin}$ is just the hopping reduction factor τ. For $N=2$, $F_{|l\rangle}^{\rm kin}$ vanishes, except in the state $|Sb\rangle$, for which, defining θ^* like θ in Table I, but using the renormalized interactions, we obtain

$$F_{|Sb\rangle}^{\rm kin}=\frac{\tau\sin(2\theta^*)}{\sin(2\theta)}.\tag{32}$$

To measure the relation between the charge and the phonon number on each site (related to the polarizability of the medium), Ref. 13 introduced, for the case of one electron, the ''electron-phonon CF.'' In our case it has to be defined as

$$F_{jk}^{\rm ep}\equiv\langle\langle n_j b_k^\dagger b_k\rangle\rangle\quad(j,k=1,2).\tag{33}$$

As k can coincide or not with j, we will consider both on-site ($j=k$) and intersite ($j\neq k$) electron-phonon CF's. The intersite charge CF is defined as $\frac{1}{4}\langle\langle n_1n_2\rangle\rangle$, and the longitudinal and transverse spin CF's are $\langle\langle S_1^zS_2^z\rangle\rangle$ and $\langle\langle S_1^-S_2^+\rangle\rangle$, respectively. The *bipolaron* ''mobility'' or *singlet-superconductor* CF (Ref. 20) describes the hopping of two particles occupying the same site, namely,

$$\begin{aligned}\langle\langle(c_{2\downarrow}c_{2\uparrow}c_{1\uparrow}^\dagger c_{1\downarrow}^\dagger)\rangle\rangle&=\langle\Psi_{\rm sq}|\mathrm{Ch}[4\gamma_0\delta(b^\dagger-b)]|\Psi_{\rm sq}\rangle\\&\quad\times\langle l|c_{2\downarrow}c_{2\uparrow}c_{1\uparrow}^\dagger c_{1\downarrow}^\dagger|l\rangle\\&=\tau^4\langle l|c_{2\downarrow}c_{2\uparrow}c_{1\uparrow}^\dagger c_{1\downarrow}^\dagger|l\rangle.\end{aligned}\tag{34}$$

Finally, the (phonon-induced) average charge transfer is defined, following Ref. 16, as

$$\begin{aligned}F_{|l\rangle}^{\rm CT}&\equiv\frac{\langle\langle(n_1-n_2)(b^\dagger+b)\rangle\rangle_{|l\rangle}}{\sqrt{\langle\langle(b^\dagger+b)^2\rangle\rangle_{|l\rangle}}}\\&=\frac{-2\delta\gamma_0\langle l|(n_1-n_2)^2|l\rangle}{\sqrt{\mathrm{Ch}(4\alpha)+4\delta^2\gamma_0^2\langle l|(n_1-n_2)^2|l\rangle}}.\end{aligned}\tag{35}$$

The analytical expressions of various CF's are collected in Table II.

V. RESULTS

The ground state of $H_{\rm pol}$ for several values of g_0 was identified by searching the minimum of the total, i.e., electronic plus phononic, energy upon independent, and simultaneous optimization of the parameters that define the shape of the orbitals (Γ), the displaced-oscillator strength (δ), and the squeezing-effect strength (α). Given α and δ, then the optimal hopping reduction factor $\tau\equiv\exp(-2\delta^2\gamma_0^2e^{-4\alpha})$ follows. Specifically, the optimization proceeded in three steps. First, the total energy for each eigenvalue was separately optimized with respect to Γ,δ, and α. Second, the minimal total energy was selected with the corresponding values of the variational parameters. Third, the higher-lying eigenvalues were recalculated with Γ,δ, and α set by the optimiza-

TABLE II. Analytic expressions of some correlation functions $\langle\langle X\rangle\rangle$ in the indicated eigenstates.

X	$\|1\sigma\rangle$	$\|Sb\rangle$	$\|T,\pm1\rangle$	$\|T,0\rangle$	$\|\mathrm{CT}\rangle$
$n_j b_j^\dagger b_j$ $(j=1,2)$	$\frac{1}{4}[\sinh^2(2\alpha)+\gamma_0^2(1+\delta)^2]$	$\frac{1}{4}\sinh^2(2\alpha)+\gamma_0^2+\gamma_0^2\delta(2+\delta)\sin^2\theta$	$\frac{1}{4}\sinh^2(2\alpha)+\gamma_0^2$	$\frac{1}{4}\sinh^2(2\alpha)+\gamma_0^2$	$\frac{1}{4}\sinh^2(2\alpha)+\gamma_0^2(1+\delta)^2$
$n_j b_k^\dagger b_k$ $(j\neq k=1,2)$	$\frac{1}{4}[\sinh^2(2\alpha)+\gamma_0^2(1-\delta)^2]$	$\frac{1}{4}\sinh^2(2\alpha)+\gamma_0^2-\gamma_0^2\delta(2-\delta)\sin^2\theta$	$\frac{1}{4}\sinh^2(2\alpha)+\gamma_0^2$	$\frac{1}{4}\sinh^2(2\alpha)+\gamma_0^2$	$\frac{1}{4}\sinh^2(2\alpha)+\gamma_0^2(1-\delta)^2$
$\frac{1}{4}n_1n_2$	0.0	$\frac{1}{4}\cos^2\theta$	$\frac{1}{4}$	$\frac{1}{4}$	0.0
$S_1^zS_2^z$	0.0	$-\frac{1}{4}\cos^2\theta$	$\frac{1}{4}$	$-\frac{1}{4}\cos^2\theta$	0.0
$S_1^-S_2^+$	0.0	$-\frac{1}{2}\cos^2\theta$	0.0	$-\frac{1}{2}$	0.0
$c_{2\downarrow}c_{2\uparrow}c_{1\uparrow}^\dagger c_{1\downarrow}^\dagger$	0.0	$\frac{1}{2}\tau^4\sin^2\theta$	0.0	0.0	$-\frac{1}{2}\tau^4$
$\dfrac{(n_1-n_2)(b^\dagger-b)}{\sqrt{\langle\langle(b^\dagger-b^2)\rangle\rangle}}$	$\dfrac{-2\delta\gamma_0}{\sqrt{\cosh(4\alpha)+(2\delta\gamma_0)^2}}$	$\dfrac{-16\delta\gamma_0\sin^2\theta}{\sqrt{\cosh(4\alpha)+(4\delta\gamma_0\sin\theta)^2}}$	0.0	0.0	$\dfrac{-16\delta\gamma_0}{\sqrt{\mathrm{c0sh}(4\alpha)+(4\delta\gamma_0)^2}}$

tion of the lowest-lying one. This procedure gave us the true full spectrum of eigenvalues for each ground state. We will now discuss the results for $N=1$ (quarter-filled case) and $N=2$ (half-filled case).

A. Quarter-filled case

The interplay between the electronic and phononic subsystems is evidenced in Fig. 1, which shows $a\Gamma,\delta$, and $\exp(-4\alpha)$ as functions of a, for $g_0=0.447$ eV and $\hbar\Omega=0.1$ eV. The displacement parameter δ grows smoothly with a, until, at a critical length $a_c\approx2.1$ Å, it jumps discontinuously up to $\delta\simeq1$. The squeezing-related quantity $\exp(-4\alpha)$ decreases with a up to a_c, indicating that the squeezing effect becomes stronger to counteract the growing displacement. At $a=a_c$, $\exp(-4\alpha)$ recovers abruptly a rather large value. The orbital-shape parameter $a\Gamma$ rises almost linearly with a, except around a_c, where it suffers a small, sharp increase. Therefore, for $N=1$, the changes of the phononic parameters have only a small effect on Γ.

The changes in the electron and phonon subsystems depicted in Fig. 1 are mirrored by the correlation functions shown in Fig. 2. We notice that the discontinuities in δ and $\exp(-4\alpha)$ at a_c correspond to the localization of the polaron, as signaled by the fact that for $a=a_c$ the kinetic energy vanishes (discontinuously) and the on-site electron-phonon correlation jumps to a very high value. The localization is driven by $\tau=\exp[-2\delta^2\gamma_0^2e^{-4\alpha}]$, which renormalizes the effective hopping [see Eq. (27)]. The sudden changes observed in Fig. 1 can be attributed to the competition between the squeezing effect, which tends to keep τ finite through the factor $e^{-4\alpha}$, and the polaron effect, which tends to reduce τ through the factor δ^2 in the exponent of τ. As δ increases with a (Fig. 1), α also increases to gain electronic energy by keeping t at a nonvanishing value (see Table I). The price to pay is an increase of the phonon energy, Eq. (28). The behavior shown for $a\leqslant a_c$ by all quantities in Fig. 2 clearly reflects the continuous variations of the phononic parameters of Fig. 1. When the phonon energy becomes too large, at $a=a_c$, the system jumps to a state with a small α and zero hopping. However, if the *bare* hopping amplitude is by itself small (which happens for large values of a), the loss in electronic energy when t is reduced is not very important, α

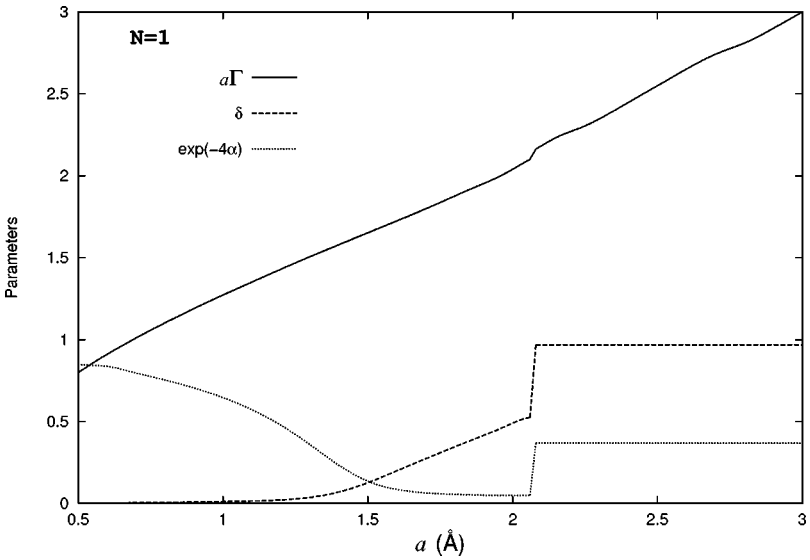

FIG. 1. The Wannier-function-shape parameter $a\Gamma$, the displaced-oscillator parameter δ, and the squeezing parameter $\exp(-4\alpha)$ as functions of a, for $N=1$, $\hbar\Omega=0.1$ eV, and $g_0=0.447$ eV.

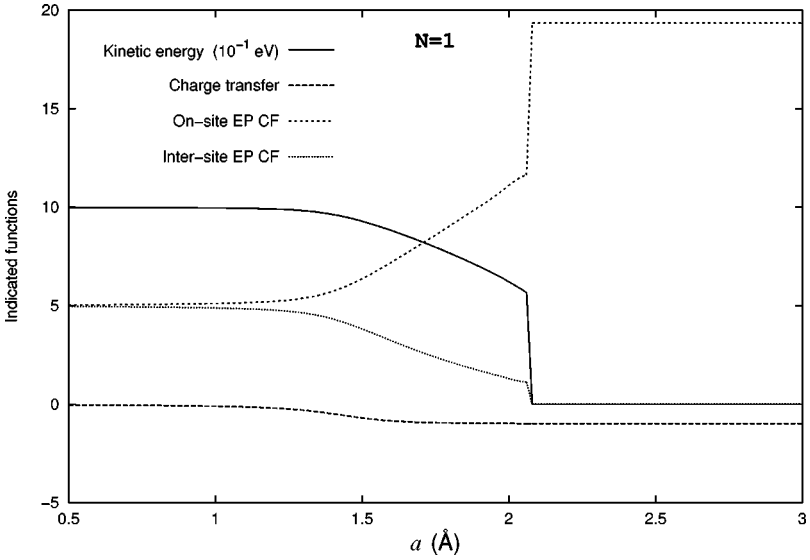

FIG. 2. Variation of the reduced kinetic energy, the charge transfer, and the on-site and intersite EP CF's with a, for $N=1$, $\hbar\Omega=0.1$ eV, and $g_0=0.447$ eV.

remains small, and there is no sudden change of state. This can be seen in Fig. 3, where the kinetic energy and the electron-phonon correlation functions are plotted as functions of g_0 for two values of a, the large-a case showing a continuous transition.

The localization critical length depends on the strength of the electron-phonon interaction. We can then draw a ''phase-diagram'' for the system, as shown in Fig. 4. In both panels, the region to the left (right) of each line corresponds to itinerant (localized) states. On the left panel we have chosen to plot the bare hopping parameter t, calculated at a_c, as a function of g_0. We also show, on the right, that $g_0^2/\hbar\Omega$ is a good scaling variable for not too large dimer lengths, as the curves for different phonon frequencies coincide. For large a, the curves tend to separate, enhancing the curvature so as to avoid crossing the x axis. This implies that the polaronic transition as a increases becomes a continuous crossover for small values of g_0.

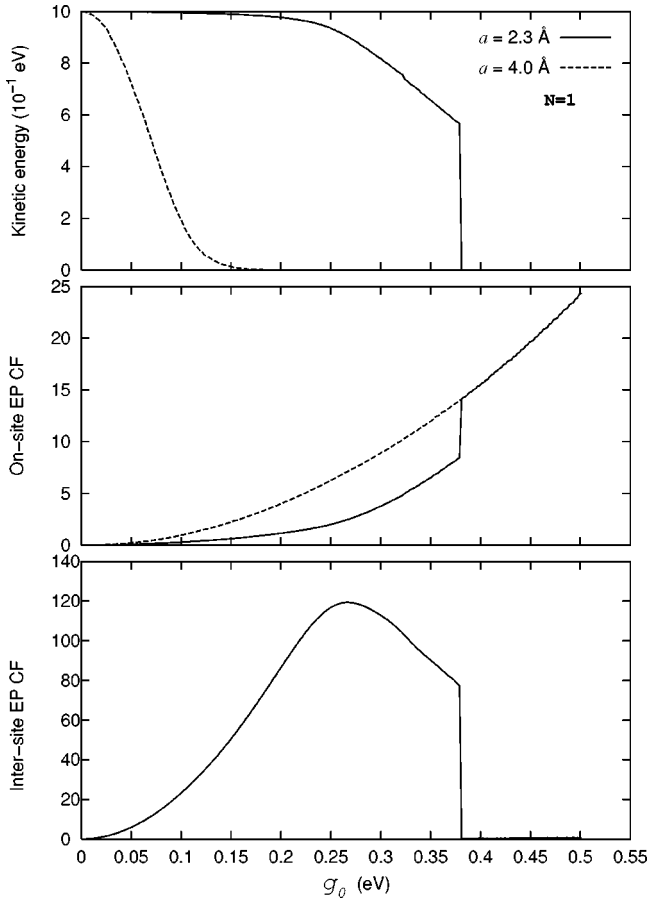

FIG. 3. The same quantities as in Fig. 2 as functions of g_0, for fixed length values $a=2.3$ Å and $a=4.0$ Å. The intersite EP CF for $a=4.0$ Å has vanishingly small values on the scale of the figure.

B. Half-filled case

The half-filled case presents a more complex behavior than the quarter-filled one, due to the electron-electron interactions that become effective in this case. We first discuss the ''phase diagram,'' Fig. 5, in order to give an overall view of the physics. Again there are two dominant regimes, localized and nonlocalized, respectively, above and below the continuous line in Fig. 5. The physics of the system is dominated by the singlet bonding state $|Sb\rangle$ (see Table I), which is always the lowest-lying energy level. However, for large a $|Sb\rangle$ becomes degenerate with either the triplet states $|T\rangle$ (Fig. 6, top panel) or the charge transfer states $|\mathrm{CT}\rangle$ (Fig. 6, middle and bottom panels), depending on the value of g_0. These degeneracies just mean that these states are no longer appropriate to describe the system, which has become a pair of isolated atoms. For small g_0, as the dimer length increases, the system evolves continuously from an extended singlet state to a localized state with one electron per site, which occurs for very large values of a. For large g_0 a bipolaron is formed (in the $|\mathrm{CT}\rangle$ state), which eventually localizes in one of the sites, leaving the other one empty.

While one can draw an Ω-independent phase diagram, the correlation functions do depend on Ω. We have therefore selected $\hbar\Omega=0.1$ eV, which might be realistic in HTSC's and colossal magnetoresistance materials. We will present the results for $g_0^2/\hbar\Omega=2.0$, 2.2, and 2.5 eV, corresponding to $g_0=0.447$, 0.470, and 0.500 eV, respectively. The dotted horizontal lines in Fig. 5 visualize the sections of the phase diagram that we are going to discuss in detail in Fig. 6, where the full eigenvalue spectrum is shown as a function of

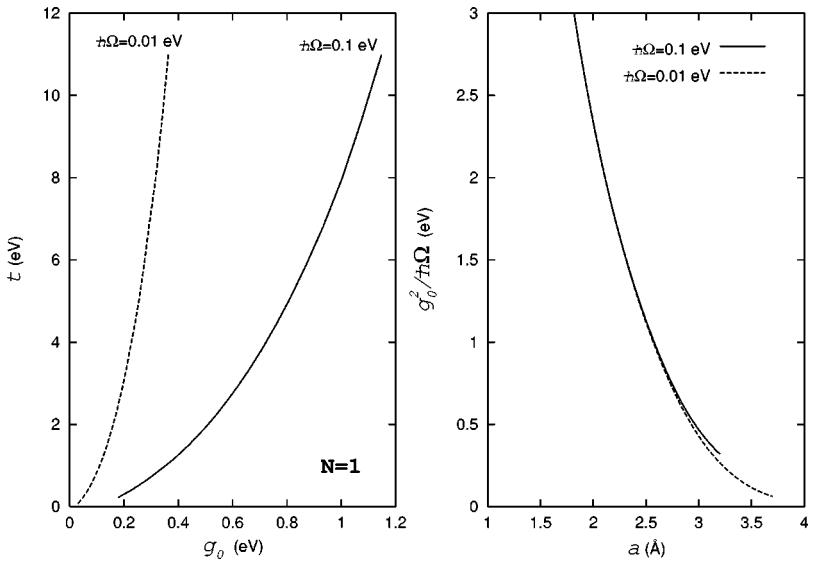

FIG. 4. The ''phase diagram'' for $N=1$ and two values of $\hbar\Omega$. The vertical coordinate is the bare hopping parameter t, and the horizontal one is the electron-phonon coupling g_0 (left panel). The electron is itinerant on the left of each curve, and localized on the right. The right panel shows that $g_0^2/\hbar\Omega$ is a good scaling variable for small a, as the two curves coincide.

a for the three mentioned values of g_0. When $g_0^2/\hbar\Omega = 2.0$ eV, $|Sb\rangle$ is always the ground state, with the $|T\rangle$ state approaching it asymptotically for large a (top panel of Fig. 6). For $g_0^2/\hbar\Omega = 2.2$ eV, we find a reentrant behavior in a range of values of a in which a rearrangement of the full spectrum occurs. Finally, in the case $g_0^2/\hbar\Omega = 2.5$ eV one crosses the region of the phase diagram in Fig. 5 bounded by the broken line, where, as we will see below, both the (antiferro)magnetic CF and the charge transfer have large values in the $|Sb\rangle$ state. Correspondingly, one sees from the bottom panel of Fig. 6 that inside this CT-AF region the state $|\mathrm{CT}\rangle$ becomes lower in energy than $|T\rangle$.

The changes in the electronic and phononic parameters underlying the level crossing in Fig. 6 are shown in Fig. 7. In

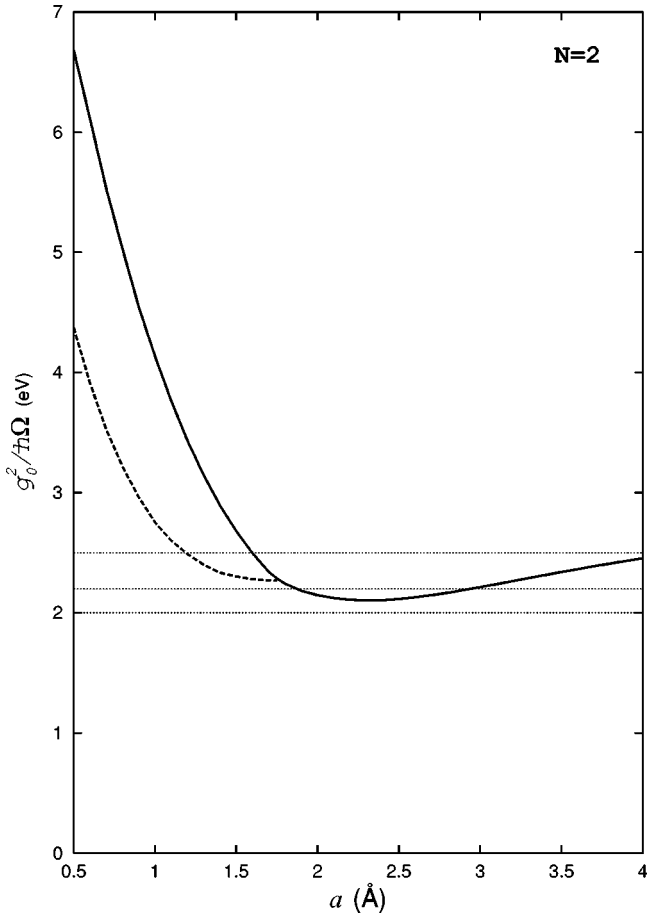

FIG. 5. The ''phase diagram'' for $N=2$. The electrons are nonlocalized below the full line, and localized in the region above it. The broken line delimits the region where both the magnetic CF and the CT are large. The horizontal lines correspond (for $\hbar\Omega = 0.1$ eV) to the values of $g_0^2/\hbar\Omega$ considered in the numerical analysis.

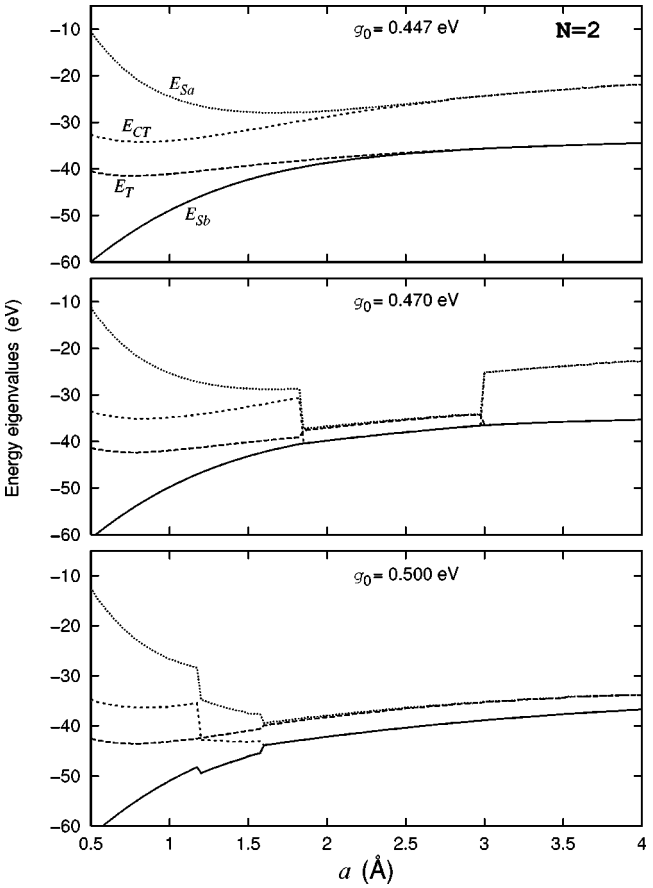

FIG. 6. Dependence of the full eigenvalue spectrum for $N=2$ with a, for $\hbar\Omega = 0.1$ eV, and the indicated values of g_0.

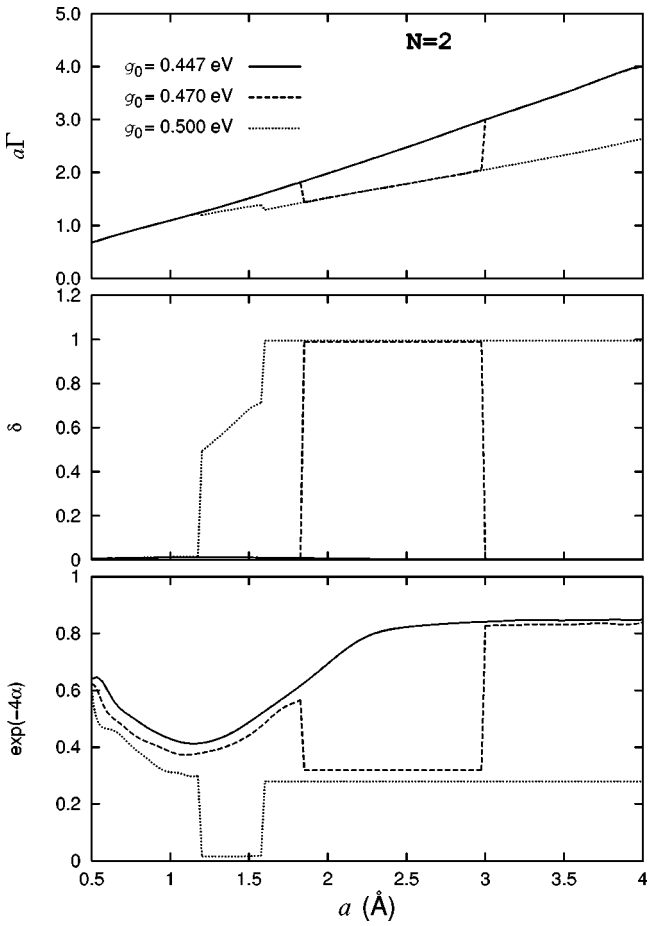

FIG. 7. Microscopic electronic and phononic parameters for $N=2$ vs a for the indicated values of g_0. Top: the Wannier wave-function shape parameter $a\Gamma$; middle: the oscillator displacement δ; bottom: the squeezing parameter $\exp(-4\alpha)$.

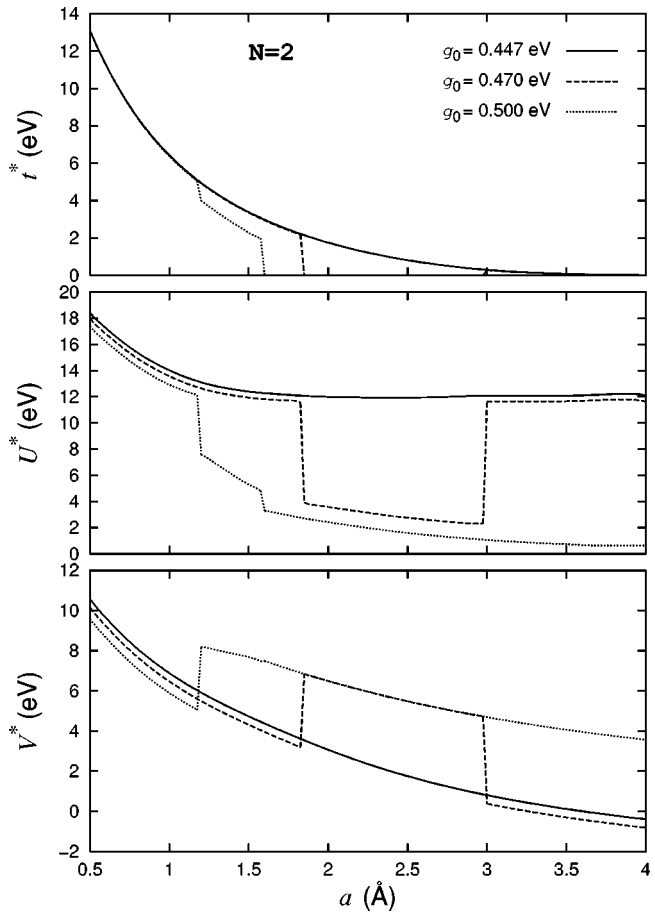

FIG. 8. The effective hopping parameter t^* (top), the on-site interaction U^* (middle), and the intersite interaction V^* (bottom) as functions of a, for $N=2$, $\hbar\Omega=0.1$ eV, and the indicated values of g_0.

the top panel $a\Gamma$ shows an approximately linear trend, steeper for $g_0^2/\hbar\Omega=2.0$ eV than for $g_0^2/\hbar\Omega=2.5$ eV. This can be explained by anticipating that, in the latter case, even when, for $a<1.60$ Å, the stable state is $|Sb\rangle$, still there is an appreciable charge transfer, indicating that the electrons tend to keep apart. Their charge-density clouds can, therefore, spread out more largely around the ions (i.e., Γ can decrease) without too much increase in the Coulomb energy. In the intermediate case $g_0^2/\hbar\Omega=2.2$ eV, $a\Gamma$ jumps between the two lines. The jumps mark the reentrant transition between the localized and the nonlocalized regime, which therefore implies marked modifications in the Wannier functions shape. The middle panel shows the corresponding behavior of the phonon displacement parameter δ. We see that the passage from the nonlocalized regime to the localized one is accompanied, as expected, by an abrupt jump from $\delta\simeq 0$ to $\delta\simeq 1$. Only for $g_0^2/\hbar\Omega=2.5$ eV is the limiting value $\delta=1$ reached by two jumps connected by a range of gradual increase, associated with the crossing of the CT-AF region in Fig. 5. The behavior of the squeezing-related parameter $\exp(-4\alpha)$, shown in the bottom panel, is also characterized by sudden transitions at the line boundaries. Its dependence on a, combined with the negligible value that δ takes when $|Sb\rangle$ is the nondegenerate ground state, implies the existence of a threshold value for $g_0^2/\hbar\Omega$ below which the electrons influence the phonons, but the converse is not true, in the sense that the latter are completely screened out, even though g_0 is not small. Large δ values in the $|Sb\rangle$ state can only be found in the CT-AF region, which, however, is located above the threshold.

In Fig. 8 we show the three largest effective electronic interactions t^*, U^*, and V^* (top, middle, and bottom panel, respectively), for the chosen values of g_0. Besides showing sharp discontinuities at the critical values of a, their behavior clarifies the nature of the CT-AF region of the phase diagram. Indeed, we can see that this region is characterized by a significant reduction of the on-site effective Coulomb repulsion and an increase of the intersite one, which are necessary conditions for the stabilization of a local bipolaron, while the effective hopping is only slightly reduced. Concomitantly, the bipolaron mobility remains finite (Fig. 9, bottom panel) while charge-transfer fluctuations build up (Fig. 10, top panel), and the intersite spin (or magnetic) correlations are still important (Fig. 10, bottom panel). We would like to remark that the existence of this region of the phase diagram (probably the most interesting one as far as high-T_c superconductors are concerned) depends strongly on the squeezing of the phonon states, as can be seen in the bottom panel of Fig. 7. In other words, the squeezing effect counteracts the oscillator displacement, and succeeds in preserving a

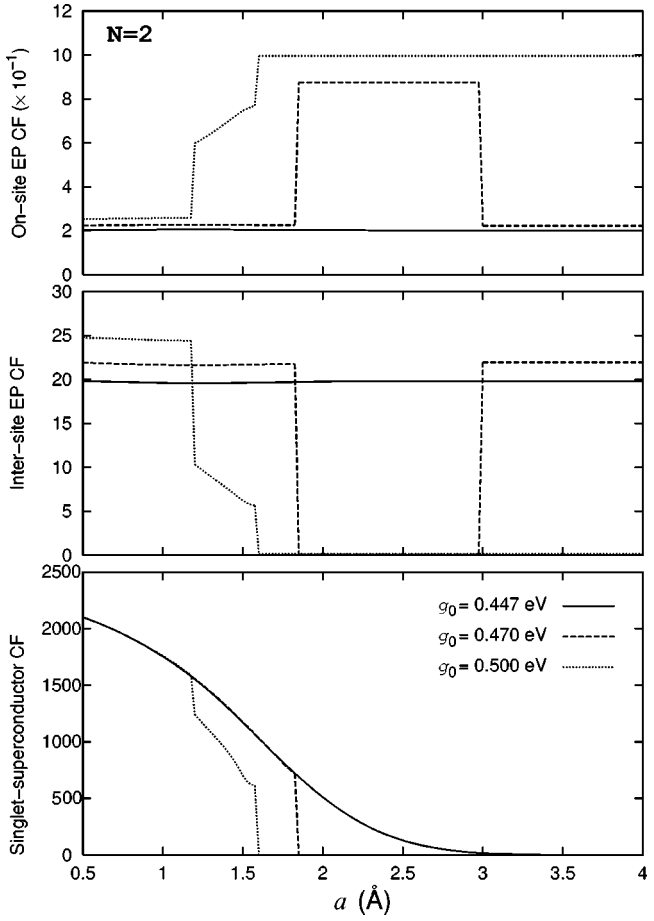

FIG. 9. The on-site electron-phonon CF (top), the intersite electron-phonon CF (middle), and the singlet-superconductor CF (bottom) as functions of a, for $N=2$, $\hbar\Omega=0.1$ eV, and the indicated values of g_0.

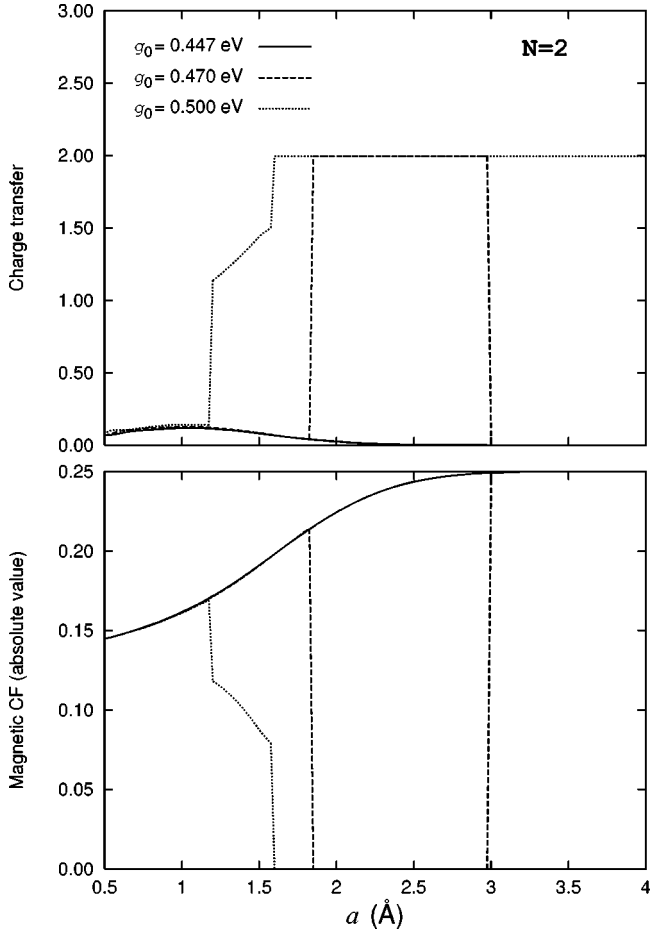

FIG. 10. The charge transfer (top) and the absolute value of the magnetic CF, $|\langle\langle S_1^z S_2^z\rangle\rangle|$, (bottom) vs a, for $N=2$, $\hbar\Omega=0.1$ eV, and the indicated values of g_0.

rather itinerant character even in the presence of both appreciable charge transfer and magnetic correlations.

VI. CONCLUSIONS

We have presented here a variational study of a dimer where interacting electrons occupy a single orbital per site and are coupled to Holstein phonons. We have put into evidence that the variation of the dimer length and/or the strength of the electron-phonon coupling yield a strong renormalization of the interaction constants as well as the width of the Wannier functions describing the local orbitals, which establishes a link between the electronic interactions and the phonons at a deeper level than predicted by the standard polaron approach. The squeezing of the phonon states has been shown to be particularly relevant, yielding sharp changes in the state of the system as the dimer length is varied at fixed electron-phonon coupling. The experimental interest of this finding is that situations where the interatomic distances can be varied, even by a small amount, either uniformly by an external pressure, or inhomogeneously by dimerization in a chain compound, can lead to important changes in the system's behavior.

Obviously one has to be careful in making predictions about the behavior of an extended system based on calculations for a two-site cluster. Nevertheless, despite the fact that Figs. 4 and 5 cannot be viewed as *phase diagrams*, we believe that they allow us to speculate on the nature of the corresponding states in a lattice. Remaining in the half-filled case, the region where the extended bonding singlet is stable should show the antiferromagnetic order characteristic of the usual Hubbard model, with a continuous evolution towards a local-moment paramagnet as the interatomic distance is increased. For a doped system, one could expect the two-site singlets to build up a RVB-like state, or an intersite bipolaron, in the lattice. On the other hand, the $|\mathrm{CT}\rangle$ state should correspond to a charge density wave in the lattice. In connection to the HTSC materials, our most significant finding is that there is a region in the parameter space where the kinetic energy, the charge transfer, and the magnetic correlations are simultaneously large, while the phonon state is partially displaced and strongly squeezed. This result suggests that it is perhaps not necessary to set a sharp alternative between either magnetic or charge instabilities. Based on our results, one might speculate that, in the normal state, those materials might be in a situation corresponding to the one in the dimer, where both types of fluctuations can be simultaneously large. It is interesting to notice that the existence of this narrow region (between the dashed and continuous lines in Fig. 5) in our model is entirely due to the squeezing of the phonon states. Indeed, we checked that it disappears if one keeps the squeezing parameter α fixed at zero, giving rise to

a direct transition from the extended singlet ground state ($\delta \approx 0.0$) to the charge transfer one ($\delta = 1.0$). We thus suggest that the competition between magnetic and charge instabilities in HTSC materials might be driven by electron-phonon interactions in the presence of strongly squeezed phonon states. It would be interesting to use the dimer solutions obtained here as building blocks for lattice states, with the aim of obtaining quantitative support for our qualitative analysis of the lattice case. Work along these lines is now in progress.

ACKNOWLEDGMENTS

We would like to thank J. Spałek, W. Wójcik, A. Painelli, S. Ciuchi, and H. Zheng for many stimulating discussions. The present work was financially supported under a CNR(Italy)-CNPq(Brazil) scientific agreement, Grant No. 910119/93-7, and by the Brazilian agency CAPES-MEC. M.A. was also partially supported by Istituto Nazionale per la Fisica della Materia (INFM), Italy, and CAPES-MEC, Brazil.

[1] J. M. Honig, H. V. Keer, G. M. Joshi, and S. A. Shivashankar, Bull. Mater. Sci. **3**, 141 (1981), and references therein.

[2] D. K. Campbell, J. Tinka Gammel, and E. Y. Loh, Phys. Rev. B **42**, 475 (1990).

[3] D. Mukhopadhyay, G. W. Haiden, and Z. G. Soos, Phys. Rev. B **51**, 9476 (1995).

[4] S. Ishihara, T. Egami, and M. Tachiki, Phys. Rev. B **49**, 8944 (1994).

[5] H. Yoshizawa, R. Kajimoto, H. Kawano, Y. Tomioka, and Y. Tokura, Phys. Rev. B **55**, 2729 (1997); Y. Moritomo, H. Kuwahara, Y. Tomioka, and Y. Tokura, *ibid.* **55**, 7549 (1997).

[6] For a recent review, see T. Egami and S. J. L. Billinge, in *Physical Properties of High Temperature Superconductors*, edited by D. M. Ginsberg (World Scientific, Singapore, 1996), Vol. V.

[7] A. Bianconi, N. L. Saini, A. Lanzara, M. Missori, T. Rossetti, H. Oyanagi, H. Yamaguchi, K. Oka, and T. Ito, Phys. Rev. Lett. **76**, 3412 (1996), and references therein; J. Zaanen and A. M. Oleś, Ann. Phys. (Leipzig) **5**, 224 (1996).

[8] J. B. Goodenough and J.-S. Zhou, Phys. Rev. B **49**, 4251 (1994).

[9] A. Kawabata, Prog. Theor. Phys. **56**, 717 (1976).

[10] J. Spałek and W. Wójcik, Phys. Rev. B **45**, 3799 (1992).

[11] A. S. Alexandrov and N. Mott, *Polarons and Bipolarons* (World Scientific, Singapore, 1995); M. Acquarone, in *High Temperature Superconductivity: Models and Measurements*, edited by M. Acquarone (World Scientific, Singapore, 1996), pp. 171–233.

[12] J. Ranninger and U. Thibblin, Phys. Rev. B **45**, 7730 (1992); E. V. L. de Mello and J. Ranninger, *ibid.* **55**, 14 872 (1997).

[13] G. Wellein, H. Roder, and H. Fehske, Phys. Rev. B **53**, 9666 (1996).

[14] J. Hubbard, Proc. R. Soc. London, Ser. A **281**, 401 (1964).

[15] A. Gołębiewski and J. Mrozek, Int. J. Quantum Chem. **7**, 623 (1973); **7**, 1021 (1973).

[16] Zheng Hang, Solid State Commun. **65**, 731 (1988); Z. Phys. B **82**, 363 (1991).

[17] The squeezing-induced zero-point energy increase that we find does not conflict with the phonon softening effect discussed, for example, by D. Feinberg, S. Ciuchi, and F. De Pasquale [Int. J. Mod. Phys. B **4**, 1317 (1990)], because our Ω^* is not the renormalized phonon frequency in the sense employed there.

[18] J. Spałek, A. M. Oleś, and K. A. Chao, Phys. Status Solidi B **108**, 329 (1981).

[19] J. de Boer and A. Schadschneider, Phys. Rev. Lett. **75**, 4298 (1995).

[20] D. M. Luz and R. R. dos Santos, Phys. Rev. B **54**, 1302 (1996).